THE JOURNAL OF PHYSICAL CHEMISTRY B

Article

Cite This: J. Phys. Chem. B 2018, 122, 3008−3014

pubs.acs.org/JPCB

Hydrophobic Collapse Initiates the Poly(*N*-isopropylacrylamide) Volume Phase Transition Reaction Coordinate

Tsung-Yu Wu, Alyssa B. Zrimsek, Sergei V. Bykov, Ryan S. Jakubek, and Sanford A. Asher*

Department of Chemistry, University of Pittsburgh, Pittsburgh, Pennsylvania 15260, United States

Supporting Information

ABSTRACT: The best-known examples of smart, responsive hydrogels derive from poly(*N*-isopropylacrylamide) (PNIPAM) cross-linked polymer networks. These hydrogels undergo volume phase transitions (VPTs) triggered by temperature, chemical, and/or environmental changes. PNIPAM hydrogels can undergo more than 50-fold volume changes within ∼1 μs intervals. Studies have tried to elucidate the molecular mechanism of these extraordinarily large responses. Nevertheless, the molecular reaction coordinates that drive the VPT remain unclear. Using visible nonresonance Raman temperature-jump spectroscopy, we determined the molecular ordering of this VPT. The PNIPAM hydrophobic isopropyl and methylene groups dehydrate with time constants of 109 ± 64 and 104 ± 44 ns, initiating the volume collapse of PNIPAM. The subsequent dehydration of the PNIPAM amide groups is significantly slower, as our group previously discovered (360 ± 85 ns). This determination of the ordering of the molecular reaction coordinate of the PNIPAM VPT enables the development of the next generation of super-responsive materials.

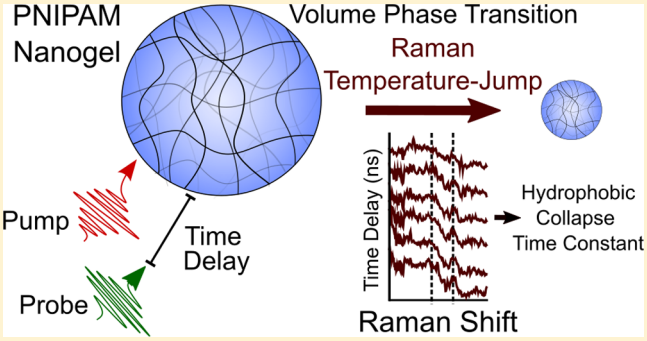

INTRODUCTION

The development of smart responsive materials will revolutionize processes that involve biomaterials, bioengineering, and chemical sensing. Smart materials can be designed to reversibly or irreversibly respond to changes in their physical or chemical environments.[1−11] These responses can be used to actuate new chemistries that enhance human well-being through tissue engineering and drug delivery, or to prevent the negative impacts of hazardous chemicals.

The most responsive smart materials, at present, are hydrogels whose large volume responses involve motion of their water mobile phase within their swollen cross-linked polymer networks. These hydrogels undergo volume phase transitions (VPTs) where the polymer network responds to physical or chemical changes, such as temperature, to expel or imbibe the mobile phase, resulting in dramatic volume changes.

Poly(*N*-isopropylacrylamide) (PNIPAM) hydrogels show the largest thermoresponsive VPT (Figure 1A). The PNIPAM hydrogel exists in a highly swollen state at temperatures below its lower critical solution temperature (LCST) of ∼32 °C.[12−15] Increasing the temperature above the LCST causes the polymer to undergo a rapid VPT that expels water, forming a dehydrated state. PNIPAM has one of the largest and fastest VPT showing up to a 50-fold volume change within ∼1 μs (Figure 1B).[16]

Despite the numerous studies of the VPT of PNIPAM-like thermoresponsive materials, there has been insufficient insight into the VPT molecular mechanism to enable its optimization. The magnitude of the VPT volume change of PNIPAM has improved little since its discovery in 1956.[17] The current understanding of hydrogel VPT derives from the thermodynamic insights of Flory and Rehner[18,19] who relate changes in osmotic pressures to hydrogel cross-linking, charge localization, and the free energy of mixing of the mobile phase with the polymer network. However, this physical insight provides little information on the VPT molecular reaction coordinate.

Many vibrational spectroscopic studies have sought insight into the PNIPAM VPT mechanism(s), but until recently, the insights were extremely limited and often contradictory. For example, studies by Ramon et al. and Lai et al. concluded that the phase transition is initiated by the breaking of the amide−water hydrogen bonds.[20,21] On the other hand, S. Sun et al.[22] and B. Sun et al.[23] proposed that the hydrophobic isopropyl methyl groups and polymer backbone dehydrate first. Consequently, it remains unclear whether the hydrophilic[20,21] or hydrophobic[22,23] groups initiate the VPT. Unlike these previous studies, we utilize a direct, time-resolved, laser-induced temperature-jump (*T*-jump) spectroscopy[24−26] to unequivocally determine the reaction coordinate for the PNIPAM VPT.

Received: January 22, 2018
Revised: February 21, 2018
Published: February 26, 2018

DOI: 10.1021/acs.jpcb.8b00740
J. Phys. Chem. B 2018, 122, 3008−3014

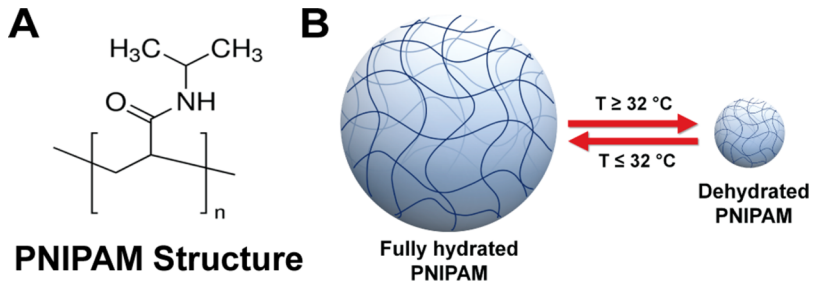

Figure 1. (A) Chemical structure of PNIPAM. (B) Schematic showing the volume phase transition of cross-linked PNIPAM hydrogel. Below the LCST, the hydrogel is in a swollen hydrated state. Above the LCST, the hydrogel is in a compact, dehydrated state.

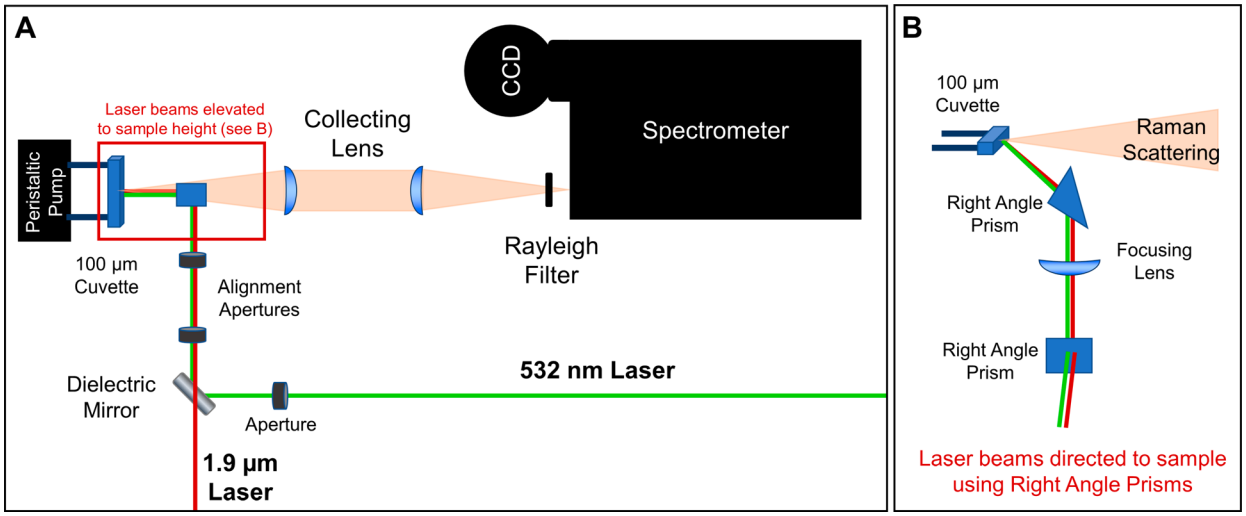

Figure 2. (A) Schematic of the nonresonance Raman *T*-jump instrument. The laser beams were directed to the 100 μm sample cuvette, as shown in part B using two turning prisms. The beams were focused onto the sample using a 12 cm focusing lens.

METHODS

PNIPAM Synthesis and Preparation. PNIPAM nanoparticles were synthesized by our previously published dispersion polymerization method,[27] where 3.4730 g of N-isopropylacrylamide (NIPAM), 0.0513 g of 2-acrylamido-2-methyl-1-propanesulfonic acid (ionic comonomer, Sigma-Aldrich), 0.1101 g of *N,N′*- methylenebis(acrylamide) (cross-linker, Fluka), 0.0815 g of sodium dodecyl sulfate (surfactant, Sigma-Aldrich), and 0.0280 g of ammonium persulfate (initiator, Sigma-Aldrich), were added to 250 mL of 18 MΩ deionized water and reacted at 70 °C for 4 h with continuous stirring. The product was filtered using glass wool and dialyzed against nanopure water by using a cellulose membrane dialysis tube (Sigma-Aldrich) for 4 weeks to remove unreacted monomer and impurities. Ionic impurities were removed by incubating the PNIPAM particles with mixed bed ion exchange resins.

PNIPAM was concentrated by centrifuging the purified suspension at 17,000 relative centrifugal force (rcf) at 34 °C for 70 min. The supernatant was removed, and the PNIPAM particles were washed with 18 MΩ deionized water to remove impurities. The PNIPAM suspension was further centrifuged at 17,000 rcf at 34 °C for 70 min. The final PNIPAM concentrations were measured to be ∼4 wt %. These concentrations were used for the 532 nm steady state Raman measurements. PNIPAM was diluted to ∼2 wt % for the *T*-jump experiments. PNIPAM particle diameters (∼0.001 wt %) were determined at different temperatures by using dynamic light scattering (DLS) (Brookhaven, ZetaPALS).

Visible Nonresonance Raman *T*-Jump and Steady State Instrumental Design. We utilized a Coherent Infinity Nd:YAG pulsed laser (3 ns pulses, 100 Hz) with a fundamental wavelength of 1064 nm. A schematic of the steady-state and *T*-jump experimental setup is shown in Figure 2. The 532 nm probe beam was generated by frequency doubling the Nd:YAG fundamental. The 1.9 μm pump beam was obtained by Raman shifting (Light Age Inc., 1000 psi, 1 m length) the 1064 nm fundamental of a second Coherent Infinity Nd:YAG laser in H_2 gas and selecting the first Stokes harmonic. Both the 532 nm and 1.9 μm beams were directed onto a dielectric mirror (Thorlabs) that reflects the 532 nm beam while transmitting the 1.9 μm beam (Figure 2A). Two apertures were used to overlap the 532 nm and 1.9 μm laser beams. The beams were directed onto the sample using a series of turning prisms and focused using a 12 cm focusing lens (Figure 2B).

We collected the Raman scattering with an ∼165° back-scattering geometry for the 532 nm steady state and *T*-jump Raman experiments. A Rayleigh rejection filter (Semrock) was placed before the slit (350 μm) to reduce the Rayleigh scattered light. The Raman scattered light was dispersed using a modified Spex single monochromator with a 500 G/mm plane ruled grating (Richardson Gratings). The dispersed light was focused on a back-thinned Princeton Instruments Pylon 1340 × 400 B CCD camera.

Visible Nonresonance Steady State Raman Measurements. Steady-state, 532 nm visible Raman spectra of

DOI: 10.1021/acs.jpcb.8b00740
J. Phys. Chem. B 2018, 122, 3008−3014

PNIPAM (~4 wt %) were measured using ~15 mW average power with an accumulation time of 20 s. PNIPAM Raman spectra were measured by using a 1 cm path length cuvette placed in a temperature controlled cuvette holder. Spectra were collected at temperatures ranging from 15 to 63 °C. The temperature of the PNIPAM sample was measured by a thermocouple placed in the sample solution.

T-Jump Raman Measurements. The *T*-jump was excited by 1.9 μm Stokes shifted Nd:YAG laser pulses that were strongly absorbed by water. To ensure that the 532 nm beam probed the sample volume that experienced the *T*-jump, the 1.9 μm *T*-jump beam was focused to a diameter (~180 μm) slightly larger than the overlapping 532 nm excitation beam (~135 μm).

For the *T*-jump measurements, a 100 μm flow cuvette (Starna Cells) is used to minimize the sample *T*-jump temperature variation along the sample thickness. A thin sample thickness is necessary because water absorbs 1.9 μm light with an absorption coefficient of 40 cm^{-1} but transmits the 532 nm Raman excitation light. Therefore, the maximum *T*-jump occurs at the front surface of the sample stream; the value of the *T*-jump decreases exponentially with sample depth. In contrast, the Raman scattering from the 532 nm beam is constant along the entire sample thickness (Figure S1A). We utilized a very thin sample thickness (100 μm) to minimize the sample *T*-jump variation along the sample thickness (Figure S1B).

Supporting Information Figure S2 shows the sample setup for the *T*-jump Raman measurements. A constant initial sample temperature was maintained by placing the PNIPAM sample solution (~2 wt %) in a stirred and heated water bath (31 °C) that was temperature controlled to ±0.1 °C (Fisherbrand Isotemp). To ensure we replace each illuminated sample volume before the next pulse, a peristaltic pump (Harvard Apparatus) flowed the sample fast enough (57 mm/s) to exchange the sample between *T*-jump pulses.

T-Jump Raman spectra were measured using 3 ns 1.9 μm pump pulses with an energy of 0.45–0.60 mJ at a 100 Hz repetition rate. The 1.9 μm *T*-jump pulse energy is sufficiently large to induce the PNIPAM VPT. The Raman 532 nm excitation beam consisted of 3 ns pulses at a 100 Hz rep rate at an average power of ~25 mW at the sample. Four 180 s accumulation Raman spectra were measured at each delay time between the *T*-jump and the Raman excitation pulses (10, 50, 100, 150, 200, 500, 750, 1000, and 5000 ns). These four spectra were averaged to improve signal-to-noise. The same method was used without the *T*-jump pulses to measure the initial temperature Raman spectra. Raman spectra were measured before and after each *T*-jump measurement to verify that the PNIPAM samples did not degrade.

Spectral Analysis. The *T*-jump magnitude was determined using the method of Lednev et al.[28] The OH Raman stretching band of water has a well-known frequency and band shape temperature dependence. We determined the water *T*-jump value from the measured water difference spectrum.

To monitor PNIPAM *T*-jump spectral changes in the CH stretching region, we subtracted PNIPAM Raman spectra collected without the 1.9 μm *T*-jump pulses (initial temperature), from Raman spectra excited with the 1.9 μm *T*-jump pulses (final temperature) at each time delay. Before subtraction, the *T*-jump Raman spectra were normalized to the intensity at the isosbestic point of the liquid water OH stretching band at ~3425 cm^{-1}.[29] The resulting peaks in the PNIPAM difference spectra were fit with mixed Gaussian and Lorentzian band shapes using the Grams AI software suite (ver. 8.0, Thermo Fisher Scientific). The PNIPAM difference peak intensities are proportional to the magnitude of the PNIPAM frequency shifts. The kinetics for the dehydration of the methylene and isopropyl methyl groups were modeled as a single exponential process.

RESULTS AND DISCUSSION

Ahmed et al. previously combined *T*-jump and UV resonance Raman (UVRR) spectroscopy to examine the temperature induced dehydration kinetics of the amide I (C═O) vibration of the PNIPAM amide groups. A 1.9 μm pump laser pulse rapidly increased the PNIPAM temperature. Then, a probe laser measured the PNIPAM UVRR response, providing time-resolved, molecular information on the heat induced VPT. They enhanced the amide I band by exciting at 204 nm, in resonance with the amide $\pi \rightarrow \pi^*$ transition. Dehydration upshifts the amide I frequency by ~28 cm^{-1}. They found that the amide groups dehydration is monoexponential with a time constant of 360 ± 85 ns.[16]

We found that UVRR cannot be used to study the side chain isopropyl methyl ($-CH(CH_3)_2$) and main chain methylene ($-CH_2-$) dehydration of PNIPAM because the UVRR enhanced amide overtones and combinations at ~2850–3000 cm^{-1} obscure the CH stretching bands (see Figure S3 in the Supporting Information). Instead, we constructed a *T*-jump nonresonance Raman instrument that utilizes 532 nm excitation to study the kinetics of PNIPAM hydrophobic group dehydration (Figure 1, Figures S1 and S2). We have accomplished, to our knowledge, the first nonresonance Raman *T*-jump measurement of PNIPAM. This method enables studies of the time-resolved structural evolution of proteins and polymers.

The PNIPAM nanogels (diameter = ~376 nm at room temperature) were characterized with dynamic light scattering (DLS). Figure 3 shows the temperature dependence of the particle diameter, as measured by DLS. The results indicate a transition temperature of ~32 °C in agreement with previous studies.[16,27,30−32] As the temperature increases from 15 to 50 °C, the particle diameter decreases from 404 to 143 nm, a 23-

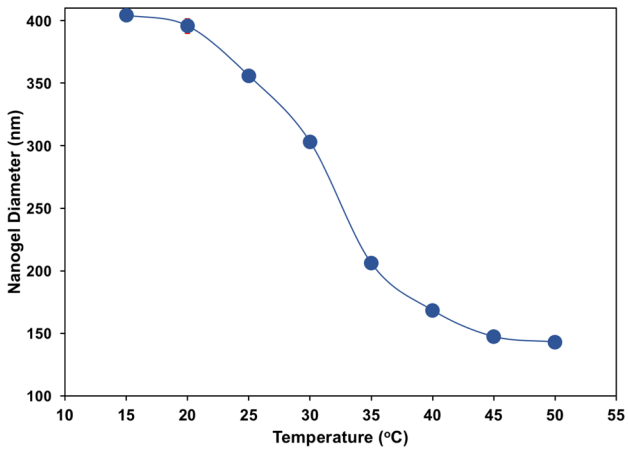

Figure 3. DLS measurements of the PNIPAM dispersion (~0.001 wt %) nanogel diameter as a function of temperature. As the temperature increases from 15 to 50 °C, the nanogel diameter decreases from 404 to 143 nm, indicating a LCST at ~32 °C.

DOI: 10.1021/acs.jpcb.8b00740
J. Phys. Chem. B 2018, 122, 3008−3014

fold volume difference. This volume change indicates that ~96 % of the PNIPAM nanogel water is expelled upon the nanogel collapse. The nanogels were also characterized by UVRR spectroscopy, as discussed in the Supporting Information, Figures S3 and S4. The UVRR results are consistent with previous studies by Ahmed et al. and others.[16,20,22,23,33]

The CH stretching band assignments for PNIPAM in the ~2850−3000 cm^{-1} region are shown in Table 1. A recent study

Table 1. Spectral Assignment of Raman Spectra of Isopropanol and Solid State PNIPAM[a]

	Raman frequency (cm^{-1})	spectral assignment	previous assignment[34]
isopropanol	2878	CH_3-FR and CH-str-gauche	2879
	2913	CH_3-FR	2911
	2916	CH_3-FR and CH-str-trans	2920
	2935	CH_3-SS	2938
	2970	CH_3-AS	2973
dehydrated solid state PNIPAM	2871	CH_2 symmetric str, CH_3-FR, and CH-str-gauche	
	2909	CH_3-FR	
	2919	CH_2 asymmetric str, CH_3-FR, and CH-str-trans	
	2937	CH_3-SS	
	2971	CH_3-AS	

[a]FR = Fermi resonance; SS = symmetric stretch; AS = asymmetric stretch.

by Yu et al. clarified the CH stretching band assignments of isopropanol.[34] These assignments include possible Fermi resonances. We used these isopropanol assignments and the PNIPAM methylene CH stretching assignments of Pimenov et al.[31] to assign the CH stretching bands. The PNIPAM spectrum matches that of isopropanol. For comparison, Raman spectra of isopropanol and solid state PNIPAM are provided in Supporting Information Figure S5. The first peak in PNIPAM at ~2871 cm^{-1} shows a slight downshift in frequency compared to that of isopropanol. This frequency shift is likely due to the presence of additional methylene group stretching from the PNIPAM backbone.[31,35] The two bands of interest for this study are highlighted in the steady state Raman spectra of PNIPAM (Figure 4A). The band at ~2917 cm^{-1} is assigned to the CH_2 antisymmetric stretching of the main chain methylene group, while the ~2976 cm^{-1} band is assigned to the CH_3 antisymmetric stretching band of the isopropyl methyl groups.

A *T*-jump induces the volume collapse of PNIPAM which evolves between a swollen and dehydrated state. The hydrophobic group dehydration during the *T*-jump gives rise to shifts in the CH stretching vibrations of PNIPAM's methylene backbone and isopropyl groups. The initial and final states of the CH stretching vibrations due to the VPT were determined from the steady state Raman spectra collected at temperatures below and above the LCST (Figure 4A). By spectroscopically monitoring the temporal evolution of the CH stretching vibrations during the *T*-jump, we can model the kinetics of the hydrophobic group dehydration. These spectral changes disclose the VPT reaction coordinate when combined with the measured amide kinetics from our previous work.[16]

The CH stretching bands of the methylene and isopropyl methyl groups shift to lower wavenumbers.[23,36] This frequency dependence on hydration was previously attributed to a

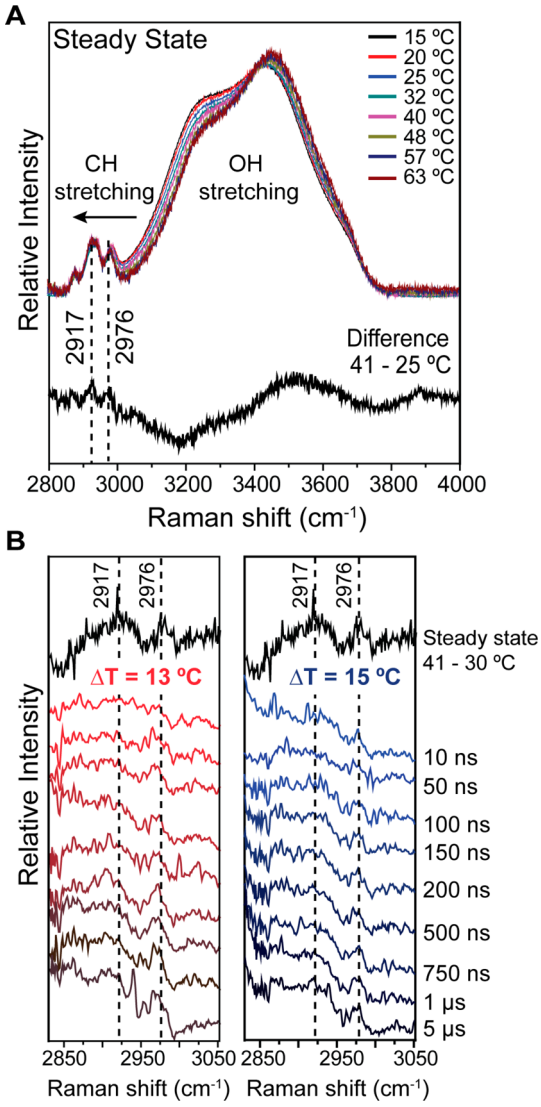

Figure 4. (A) Top: Raman spectra (532 nm excitation) of PNIPAM in H_2O at indicated steady state temperatures. Bottom: The steady state difference spectrum (41−25 °C) of PNIPAM. The frequency shifts of the CH stretching bands are due to changes in hydration of the PNIPAM isopropyl and methylene groups. (B) Left: Time-resolved 13 °C *T*-jump Raman difference spectra at indicated delay times. Right: Time-resolved, 15 °C *T*-jump Raman difference spectra at indicated delay times. The time-resolved difference spectra were calculated by subtracting the Raman spectrum of PNIPAM at its initial temperature, from the 13 °C (or 15 °C) *T*-jump heated Raman spectra measured with the indicated delay times. The steady state spectra in part B were collected identically to the *T*-jump spectra, except that the *T*-jump beam was blocked, and the samples were heated with a temperature controlled water bath.

hydrogen bonding interaction that strengthens the X−H bonds and blue-shifts their band frequencies. This type of hydrogen bonding has been referred to as "improper, blue-shifting hydrogen bonding".[35,37−39] These frequency shifts in PNIPAM are easily observed as peaks in the 41−25 °C steady state difference spectra where the difference peak intensity is proportional to the magnitude of the frequency shift (Figure 4A).

The two *T*-jump measurements (ΔT = 13 and 15 °C) with time delays between 10 and 5000 ns between the pump and probe pulses are essentially identical (Figure 4B). The *T*-jump

DOI: 10.1021/acs.jpcb.8b00740
J. Phys. Chem. B 2018, 122, 3008−3014

magnitude was determined using the method of Lednev et al.[28] The kinetics for the dehydration of the methylene and isopropyl methyl groups can be modeled as a single exponential process, as shown in Figure 5. We find that dehydration of the isopropyl groups occurs with an apparent time constant (τ) of 109 ± 64 ns (Figure 5A), while the methylene main chain groups show an essentially identical time constant of τ = 104 ± 44 ns (Figure 5B). Additional dehydration kinetics for the 13 and 15 °C *T*-jumps are shown in Supporting Information Figure S6.

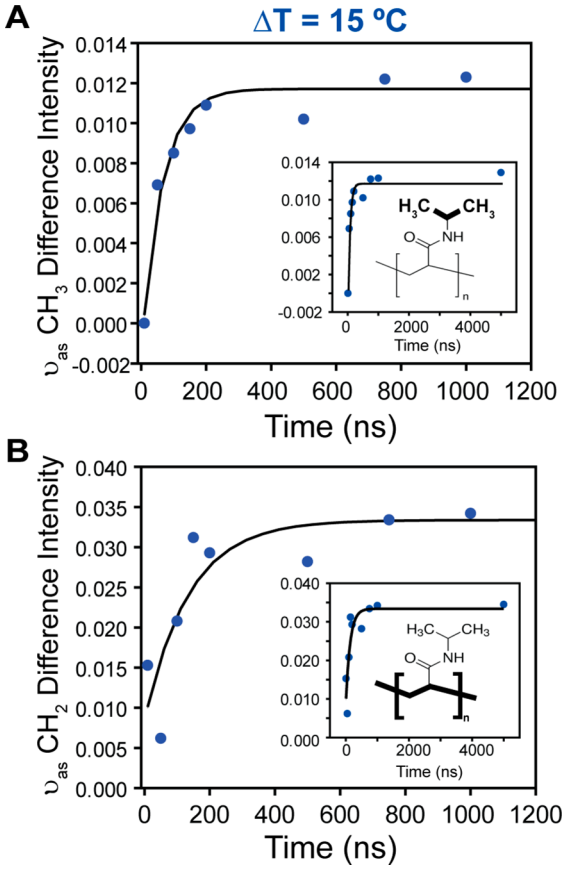

Figure 5. Kinetics of the PNIPAM isopropyl and backbone methylene group dehydration for the 15 °C *T*-jump (see the Supporting Information for the 13 °C *T*-jump). The inset shows time delays out to 5 μs. (A) Kinetics of the peak intensity difference spectra of the isopropyl CH_3 antisymmetric stretching (ν_{as}) band (~2976 cm^{-1}). The τ = 109 ± 64 ns is the average of the 13 and 15 °C *T*-jumps. (B) Kinetics of the peak intensity difference spectra of the methylene main chain CH_2 antisymmetric stretching (ν_{as}) band (~2917 cm^{-1}). The τ = 104 ± 44 ns is the average of the 13 and 15 °C *T*-jumps.

Combining our new, nonresonance Raman *T*-jump data with our previous UVRR *T*-jump data,[16] we conclude that the temperature induced PNIPAM collapse is initiated by dehydration of the hydrophobic groups via hydrophobic collapse with an average of τ = 107 ± 37 ns. This cooperative transition forces the subsequent dehydration of the side chain hydrophilic amide groups at τ = 360 ± 85 ns,[16] which expels large water clusters from the polymer network. The proposed VPT mechanism is illustrated in Figure 6. Our results directly demonstrate that the hydrophobic group collapse initiates the PNIPAM VPT in response to a *T*-jump.

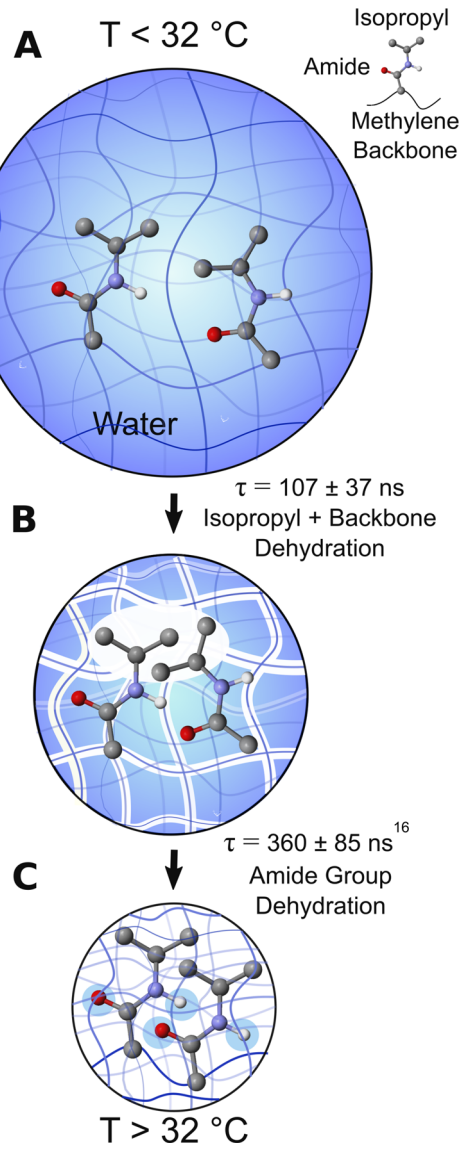

Figure 6. Illustration of the VPT of PNIPAM. (A) Below the LCST, the PNIPAM hydrogel exists in a fully hydrated state. (B) As the temperature increases, hydrophobic collapse occurs. The isopropyl groups and the methylene groups dehydrate with an average of τ = 107 ± 37 ns. (C) Subsequently, the amide groups dehydrate and water is expelled, τ = 360 ± 85 ns.[16]

CONCLUSION

In summary, we used nonresonance time-resolved Raman spectroscopy to investigate the molecular mechanism of the PNIPAM VPT and obtain the first direct measurement of the hydrophobic group dehydration kinetics. We monitor the shift in frequencies of the CH_2 antisymmetric stretching bands of the main chain methylene group and the CH_3 antisymmetric stretching bands of the isopropyl group during the VPT. As the temperature increases past the LCST, dehydration of the isopropyl groups and the main polymer chain occurs with τ = 107 ± 37 ns. This is much faster than the dehydration of the amide groups, which was previously measured to occur with τ = 360 ± 85 ns,[16] demonstrating that the hydrophobic groups initiate the PNIPAM VPT. We can utilize this new insight into the VPT reaction coordinate to engineer and optimize the PNIPAM polymer structure to increase the VPT magnitude

DOI: 10.1021/acs.jpcb.8b00740
J. Phys. Chem. B 2018, 122, 3008−3014

and response rate to fabricate more efficient, super-responsive smart materials.

■ ASSOCIATED CONTENT

Supporting Information

The Supporting Information is available free of charge on the ACS Publications website at DOI: 10.1021/acs.jpcb.8b00740.

Additional experimental methods, UVRR characterization of PNIPAM, isopropanol and solid state PNIPAM Raman spectra, and 13 and 15 °C *T*-jump kinetic data (PDF)

■ AUTHOR INFORMATION

Corresponding Author

*E-mail: asher@pitt.edu.

ORCID

Tsung-Yu Wu: 0000-0003-0600-5294

Ryan S. Jakubek: 0000-0001-7880-9422

Notes

The authors declare no competing financial interest.

■ ACKNOWLEDGMENTS

This work was supported by the Defense Threat Reduction Agency (DTRA HDTRA1-15-1-0038). We would like to thank the University of Pittsburgh Machine Shop for their advice on instrument design for our *T*-jump apparatus. We thank Charles Fleishaker for maintaining our aging lasers. S.V.B. and A.B.Z. thank the Office of Naval Research (ONR N00014-16-1-2681) for financial support.

■ REFERENCES

(1) Holtz, J. H.; Asher, S. A. Polymerized Colloidal Crystal Hydrogel Films as Intelligent Chemical Sensing Materials. *Nature* **1997**, *389*, 829−832.

(2) Ohya, S.; Nakayama, Y.; Matsuda, T. Thermoresponsive Artificial Extracellular Matrix for Tissue Engineering: Hyaluronic Acid Bioconjugated with Poly(N-isopropylacrylamide) Grafts. *Biomacromolecules* **2001**, *2*, 856−863.

(3) Oktar, O.; Caglar, P.; Seitz, W. R. Chemical Modulation Of Thermosensitive Poly(N-Isopropylacrylamide) Microsphere Swelling: A New Strategy for Chemical Sensing. *Sens. Actuators, B* **2005**, *104*, 179−185.

(4) Schmaljohann, D. Thermo-and pH-Responsive Polymers in Drug Delivery. *Adv. Drug Delivery Rev.* **2006**, *58*, 1655−1670.

(5) Kang Derwent, J. J.; Mieler, W. F. Thermoresponsive Hydrogels as a New Ocular Drug Delivery Platform to the Posterior Segment of the Eye. *Trans. Am. Ophthalmol. Soc.* **2008**, *106*, 206−214.

(6) Hendrickson, G. R.; Andrew Lyon, L. Bioresponsive Hydrogels for Sensing Applications. *Soft Matter* **2009**, *5*, 29−35.

(7) Guan, Y.; Zhang, Y. PNIPAM Microgels for Biomedical Applications: From Dispersed Particles to 3D Assemblies. *Soft Matter* **2011**, *7*, 6375−6384.

(8) Chen, K.-J.; Liang, H.-F.; Chen, H.-L.; Wang, Y.; Cheng, P.-Y.; Liu, H.-L.; Xia, Y.; Sung, H.-W. A Thermoresponsive Bubble-Generating Liposomal System for Triggering Localized Extracellular Drug Delivery. *ACS Nano* **2013**, *7*, 438−446.

(9) Wu, Z. L.; Moshe, M.; Greener, J.; Therien-Aubin, H.; Nie, Z.; Sharon, E.; Kumacheva, E. Three-Dimensional Shape Transformations of Hydrogel Sheets Induced by Small-Scale Modulation of Internal Stresses. *Nat. Commun.* **2013**, *4*, 1586.

(10) Palomino, K.; Suarez-Meraz, K. A.; Serrano-Medina, A.; Olivas, A.; Samano, E. C.; Cornejo-Bravo, J. M. Microstructured Poly(N-Isopropylacrylamide) Hydrogels with Fast Temperature Response for Pulsatile Drug Delivery. *J. Polym. Res.* **2015**, *22*, 199.

(11) Lei, Z.; Wang, Q.; Wu, P. A Multifunctional Skin-Like Sensor Based on a 3D Printed Thermo-Responsive Hydrogel. *Mater. Horiz.* **2017**, *4*, 694−700.

(12) Deshmukh, S. A.; Kamath, G.; Suthar, K. J.; Mancini, D. C.; Sankaranarayanan, S. K. R. S. Non-Equilibrium Effects Evidenced by Vibrational Spectra During the Coil-To-Globule Transition in Poly(N-Isopropylacrylamide) Subjected to an Ultrafast Heating-Cooling Cycle. *Soft Matter* **2014**, *10*, 1462−1480.

(13) Deshmukh, S. A.; Sankaranarayanan, S. K.; Mancini, D. C. Vibrational Spectra of Proximal Water in a Thermo-Sensitive Polymer Undergoing Conformational Transition Across the Lower Critical Solution Temperature. *J. Phys. Chem. B* **2012**, *116*, 5501−5515.

(14) Deshmukh, S. A.; Sankaranarayanan, S. K. R. S.; Suthar, K.; Mancini, D. C. Role of Solvation Dynamics and Local Ordering of Water in Inducing Conformational Transitions in Poly(N-isopropylacrylamide) Oligomers through the LCST. *J. Phys. Chem. B* **2012**, *116*, 2651−2663.

(15) Reese, C. E.; Mikhonin, A. V.; Kamenjicki, M.; Tikhonov, A.; Asher, S. A. Nanogel Nanosecond Photonic Crystal Optical Switching. *J. Am. Chem. Soc.* **2004**, *126*, 1493−1496.

(16) Ahmed, Z.; Gooding, E. A.; Pimenov, K. V.; Wang, L.; Asher, S. A. UV Resonance Raman Determination of Molecular Mechanism of Poly(N-isopropylacrylamide) Volume Phase Transition. *J. Phys. Chem. B* **2009**, *113*, 4248−4256.

(17) E.H. Sprecht, A. N., H.T. Neher, H. T. Preparation of Acrylamides. U.S Patent 2,773,063, Dec 4, 1956.

(18) Flory, P. J.; Rehner, J. Statistical Theory of Chain Configuration and Physical Properties of High Polymers. *Ann. N. Y. Acad. Sci.* **1943**, *44*, 419−429.

(19) Flory, P. J. *Principles of Polymer Chemistry*; Cornell University Press: Ithaca, NY, 1953.

(20) Lai, H.; Wu, P. A Infrared Spectroscopic Study on the Mechanism of Temperature-Induced Phase Transition of Concentrated Aqueous Solutions of Poly(N-Isopropylacrylamide) and N-Isopropylpropionamide. *Polymer* **2010**, *51*, 1404−1412.

(21) Ramon, O.; Kesselman, E.; Berkovici, R.; Cohen, Y.; Paz, Y. Attenuated Total Reflectance/Fourier Transform Infrared Studies on the Phase-Separation Process of Aqueous Solutions of Poly(N-Isopropylacrylamide). *J. Polym. Sci., Part B: Polym. Phys.* **2001**, *39*, 1665−1677.

(22) Sun, S.; Hu, J.; Tang, H.; Wu, P. Chain Collapse and Revival Thermodynamics of Poly(N-isopropylacrylamide) Hydrogel. *J. Phys. Chem. B* **2010**, *114*, 9761−9770.

(23) Sun, B.; Lin, Y.; Wu, P.; Siesler, H. W. A FTIR and 2D-IR Spectroscopic Study on the Microdynamics Phase Separation Mechanism of the Poly(N-isopropylacrylamide) Aqueous Solution. *Macromolecules* **2008**, *41*, 1512−1520.

(24) Weissman, J. M.; Sunkara, H. B.; Tse, A. S.; Asher, S. A. Thermally Switchable Periodicities and Diffraction from Novel Mesoscopically Ordered Materials. *Science* **1996**, *274* (5289), 959−963.

(25) Lednev, I. K.; Karnoup, A. S.; Sparrow, M. C.; Asher, S. A. A-Helix Peptide Folding and Unfolding Activation Barriers: A Nanosecond UV Resonance Raman Study. *J. Am. Chem. Soc.* **1999**, *121*, 8074−8086.

(26) Walrafen, G. E.; Hokmabadi, M. S.; Yang, W. H. Raman Isosbestic Points from Liquid Water. *J. Chem. Phys.* **1986**, *85*, 6964−6969.

(27) Eigen, M. Immeasurably Fast Reactions. *Nobel Lecture* **1967**, *11*, 1963−1979.

(28) Kubelka, J. Time-Resolved Methods in Biophysics. 9. Laser Temperature-Jump Methods for Investigating Biomolecular Dynamics. *Photochem. Photobiol. Sci.* **2009**, *8*, 499−512.

(29) Yamamoto, K.; Mizutani, Y.; Kitagawa, T. Construction of Novel Nanosecond Temperature Jump Apparatuses Applicable to Raman Measurements and Direct Observation of Transient Temperature. *Appl. Spectrosc.* **2000**, *54*, 1591−1604.

(30) Dybal, J.; Trchová, M.; Schmidt, P. The Role of Water in Structural Changes of Poly (N-Isopropylacrylamide) and Poly (N-

DOI: 10.1021/acs.jpcb.8b00740
J. Phys. Chem. B 2018, 122, 3008−3014

Isopropylmethacrylamide) Studied by FTIR, Raman Spectroscopy and Quantum Chemical Calculations. *Vib. Spectrosc.* **2009**, *51*, 44−51.
(31) Pimenov, K. V. UV Raman Investigation of Peptidehydration and Hydrophobic Collapse. MS Thesis, University of Pittsburgh, Pittsburgh, PA, 2007.
(32) Takahashi, K.; Takigawa, T.; Masuda, T. Swelling and Deswelling Kinetics of Poly(N-Isopropylacrylamide) Gels. *J. Chem. Phys.* **2004**, *120*, 2972−2979.
(33) Speer, M. Raman Spectroscopy as a Technique for Studying the Structure and Mechanism of the Volume Phase Transition of Poly (N-Isopropylacrylamide. MS Thesis, University of Pittsburgh, Pittsburgh, PA, 2013.
(34) Yu, Y.; Wang, Y.; Hu, N.; Lin, K.; Zhou, X.; Liu, S. Overlapping Spectral Features and New Assignment of 2-Propanol in the C−H Stretching Region. *J. Raman Spectrosc.* **2014**, *45*, 259−265.
(35) Snyder, R.; Hsu, S.; Krimm, S. Vibrational Spectra in the C-H Stretching Region and the Structure of the Polymethylene Chain. *Spectrochim. Acta, Part A* **1978**, *34*, 395−406.
(36) Yu, Y.; Wang, Y.; Hu, N.; Lin, K.; Zhou, X.; Liu, S. Overlapping Spectral Features and New Assignment of 2-propanol in the C−H Stretching Region. *J. Raman Spectrosc.* **2014**, *45*, 259−265.
(37) Hobza, P.; Havlas, Z. Improper, Blue-Shifting Hydrogen Bond. *Theor. Chem. Acc.* **2002**, *108*, 325−334.
(38) Schmidt, P.; Dybal, J.; Trchová, M. Investigations of the Hydrophobic and Hydrophilic Interactions in Polymer−Water Systems by ATR FTIR and Raman Spectroscopy. *Vib. Spectrosc.* **2006**, *42*, 278−283.
(39) Hobza, P.; Havlas, Z. Blue-Shifting Hydrogen Bonds. *Chem. Rev.* **2000**, *100*, 4253−4264.

DOI: 10.1021/acs.jpcb.8b00740
J. Phys. Chem. B 2018, 122, 3008−3014